



## **Advancements in CPW-Fed Antennas: Review on Design Techniques and Performance Optimization for 5G and Beyond**

**Manish Kumar<sup>1</sup>, Sandeep Kumar Singh<sup>1\*</sup>, Arvind Kumar Singh<sup>2</sup>, Tripurari Sharan<sup>3</sup>**

<sup>1</sup>Department of EEC, Sharda University, Uttar Pradesh, India

<sup>2</sup>Department of Electrical Engineering, NERIST, Nirjuli, Arunachal Pradesh, India, 791109

<sup>3</sup>Department of ECE, NERIST, Nirjuli, Arunachal Pradesh, India, 791109

*Received date: 15/05/2025, Acceptance date: 25/06/2025*

**DOI:** <http://doi.org/10.63015/10s-2464.2.3>

*\*Corresponding Author: [\\_sandeepsingh.ec@sharda.ac.in](mailto:_sandeepsingh.ec@sharda.ac.in)*

### **Abstract**

This review comprehensively explores recent advancements in coplanar waveguide (CPW)-fed antenna design, with a particular focus on performance optimization techniques applicable to 5G and future 6G wireless systems. The study investigates a wide array of design methodologies including the integration of stubs, slots, strips, corner truncation, substrate engineering, defected ground structures (DGS), defected substrates, metamaterials (MTM), frequency-selective surfaces (FSS), conductor-backed (CB) configurations, modified ground structures (MGS), metal reflectors, and MIMO architectures. A detailed parametric comparison reveals how these approaches significantly enhance key antenna parameters such as impedance bandwidth (up to 181%), gain (up to 13.1 dBi), axial ratio bandwidth, miniaturization (up to 72.7% size reduction), polarization purity, and frequency agility across multiple bands. Applications span 5G/6G mobile, biomedical, IoT, satellite, CubeSat, and vehicular systems. In particular, techniques like MIMO and metamaterial integration deliver high port isolation ( $\geq 15$  dB), ultra-wideband (UWB) support, and enhanced diversity performance. This work provides a roadmap for selecting optimal design combinations tailored to specific wireless standards and platforms. Future research is encouraged to explore reconfigurable structures, AI-driven design automation, transparent and sustainable materials, and energy-harvesting integration for next-generation intelligent antenna systems.

**Keywords:** DGS, CPW-fed, CB-CPW Antenna, CB-MTS, FSS, CPW-MIMO Antenna.

**1. Introduction:** Antennas constitute a fundamental component in wireless communication systems [1]. Over the past two decades, there has been a significant surge in the demand for compact, low-cost, flexible, and broadband antennas. However, integrating multiple antennas into a single mobile device remains a challenging task due to spatial limitations, thereby necessitating effective isolation between coexisting communication technologies. Microstrip patch antennas, widely recognized for their compactness, lightweight structure, cost-efficiency, and compatibility with integrated circuit technologies, have become increasingly relevant in modern communication systems. These antennas typically support single-mode linearly polarized (LP) waves, which are oriented either horizontally or vertically [2]. To address the limitations of LP antennas, circularly polarized (CP) antennas are being increasingly explored due to their ability to support independent data transmission and reception, mitigate multipath fading, enhance resilience in diverse environmental conditions, and improve polarization matching accuracy [3]. Several slotted patch configurations such as E, S, and H-shaped patches, dual-polarized Xi-shaped designs, and inverted L-shaped parasitic strips have been developed to improve CP antenna bandwidth in indoor wireless scenarios [4]. These designs are often adapted for fifth-generation (5G) millimeter-wave applications, supporting multiple frequency bands including Industrial, Scientific, and Medical (ISM) bands (2.4–2.485 GHz, 5.725–5.875 GHz), Wireless Local Area Network (WLAN), Worldwide Interoperability for Microwave Access (WiMAX), Bluetooth, Ultra High Frequency (UHF), and sub-6 GHz 5G bands [5]. To enhance CP antenna performance further, modifications involving parasitic elements and ground planes have also been explored. CP antennas are well-suited for Radio Frequency Identification (RFID) applications

due to their reliability and stable wireless links, with RFID technology offering advantages such as high data rates, extended range, robust security, and multi-band operability. Designing CP antenna with wide 3-dB axial-ratio bandwidths remains a persistent challenge due to their inherent size constraints [6–8]. Nonetheless, proximity feeding and other techniques have helped in achieving broadband CP antenna operation, particularly for WiMAX, WLAN, and ISM bands [9]. Moreover, CP antennas have found applications in narrowband microstrip designs on substrates like FR4 and PTFE, particularly for Dedicated Short-Range Communication (DSRC) at 5.9 GHz [10]. With the advent of advanced wireless technologies, CPW offers advantages such as low radiation loss, compactness, ease of integration with monolithic microwave integrated circuits (MMICs), and wide impedance bandwidth. These attributes are especially beneficial for compact, flexible, and high-frequency systems like 5G and 6G. Compact CPW-fed implantable antennas have been introduced for biomedical telemetry, particularly within the ISM bands of 2.45 GHz and 5.8 GHz [11–12]. Low-profile, wideband, circularly polarized CPW-fed antennas have also been proposed for biotelemetry and body-worn applications [13], while similar configurations are optimized for GNSS and RFID systems [14]. Other implementations include vehicle-mounted CP antennas that operate in upper GNSS bands (1.559–1.606 GHz) [15]. CubeSats represent a prominent area where CPW-fed printed monopole and meta surface antennas are leveraged for compact satellite communication systems [16], with additional advancements in the use of additively manufactured meta surface structures to enhance CP antenna performance in the X-band [17]. These solutions are particularly effective in inter-satellite and satellite-to-ground communication links [18]. For sub-6 GHz massive machine-type communications, asymmetric CPW-fed CP antennas have been

designed to ensure high radiation efficiency and miniaturization [19]. Moreover, optically transparent CPW antennas on glass substrates have gained traction for automotive and aesthetic integration [20]. In high-density antenna systems, mutual coupling is mitigated using strategies like defected ground structures (DGS), electromagnetic bandgap structures, and parasitic elements [21]. Novel CPW-fed antenna designs targeting wearable and super-wideband applications have been proposed, including integration with emblematic structures like the Mercedes-Benz logo, for ISM band operation within Wireless Body Area Networks (WBANs) [22]. For vehicular communication systems, a CPW-fed patch antenna designed to operate at 5.9 GHz has been developed for DSRC applications, contributing to improved safety communications [23]. Innovative antenna geometries such as Om ( $\text{Om}$ ) and double-Damru shapes fabricated on low-cost FR-4 substrates support multiband operations across S, C, and Ku-bands, including 5G systems [24, 25]. Other techniques employ inverted L-shaped elements, modified ground planes, and metamaterial loading to ensure performance across a wide frequency spectrum including GSM, Wi-Fi, WiMAX, LTE, and Ultra-Wideband (UWB) [26, 27]. Antenna arrays with  $1 \times 2$  radiating elements and integrated DGS have been utilized to support dual-band operations such as GPS, GSM, UMTS, Bluetooth, and WiMAX [28]. Similarly, compact crown-shaped CPW-fed antennas have been reported for C- and X-band communication [29]. Double-patch CPW configurations are also effective in enhancing gain and bandwidth, particularly in WLAN environments [30]. Compact broadband CPW antennas have been engineered with favorable features such as mechanical durability, rapid thermal dissipation, and low loss, making them well-suited for ISM, RFID, and WLAN systems [31]. DGS continues to play a vital role in improving gain and bandwidth across

multiple bands, notably WLAN, UWB, and WiMAX [32–34]. CPW-fed meta surface antennas, especially miniaturized ones, have been proposed for 5G [35] and UWB applications [36], while textile-based antennas are being considered for Wireless Personal Area Networks (WPAN) and biomedical use on flexible substrates [37, 38]. Finally, frequency-selective surface (FSS)-integrated CPW antenna arrays with high front-to-back ratios have been proposed for aerospace, IoT, and wideband applications [39–41]. To address interference challenges in UWB communication, antennas with band-notch characteristics have been designed, effectively suppressing WiMAX, WLAN, and satellite signal interference [42–45]. CPW-fed antennas have proven themselves to be suitable for several applications, including 5G, and have wide potential to be implemented to make 6G antennas by optimizing the antennas with different techniques and achieving the desired gain, directivity, efficiency, and bandwidth. The size of the antenna [47] can also be easily optimized to fit the desired platform and be used for a wide variety of applications. The CPW-fed patch antenna's bandwidth, Voltage Standing Wave Ratio (VSWR), gain, and radiation pattern can all be influenced by several design techniques. However, all these characteristics can be improved by carefully adjusting the substrate material, ground plane, and radiating stub, followed by some additional techniques like DGS, FSS, MTM, CB-CPW, CB-MTS CPW, and MIMO for improving gain, directivity, and efficiency, as well as antenna miniaturization for multiple applications, including 5 G. This article will undertake and optimize the following parametric studies with various design methodologies.

In the following, the article is presented in four sections. In section 2, comparative study and design techniques have been discussed. In section 3, comparative outcomes and in section 4, conclusion and future scope is given.

## 2. Comparative Study and Design Techniques:

The appropriate design techniques and the right antenna is crucial because it greatly influences the RF system's performance, including factors like bandwidth and communication range. Researchers have introduced numerous methods to enhance antenna bandwidth and gain while minimizing size. Various approaches can adjust key antenna parameters such as bandwidth, gain, directivity, efficiency, and impedance matching enabling their use in diverse applications like WLAN, Wi-Fi, WiMAX, ISM bands, C-band, X-band, Ku/Ka bands, and 5G networks. Additionally, these modifications allow antennas to operate across multiple frequency bands simultaneously, increasing their versatility.

**2.1. Effect of adding stubs, slots, strips, cutting corners:** Recent years have seen significant advancements in CP ultra-wideband antenna designs. Various techniques, such as corner-cutting, slot-loading, branch-line loading, and inverted L-shaped microstrip structures on FR4 substrates, enhance CP radiation in microstrip antennas. Annular ring slots and inverted microstrips improve impedance matching over wider frequencies, making them ideal for satellite and broadband applications [1]. To achieve right-hand (RHCP) and left-hand (LHCP) circular polarization, CPW-fed slot antennas with L-shaped strips and stubs are studied [2]. Modifications like parasitic strips and ground-plane adjustments further extend CP bandwidth [4]. Monopole antennas with square-ring slits achieve a 70% axial ratio (AR) bandwidth (2.62–5.42 GHz) [5]. This article presents a CPW-fed antenna design using various substrate materials and techniques, demonstrating tunable multi-band operation (3.3–10.1 GHz) with optimized  $|S_{11}|$ , IBW, and gain [6]. A compact CPW-fed antenna with slotted patch and stub-loaded DGS achieves super wideband performance (1.21–24.66 GHz) and 9.4 dB gain, making it suitable for microwave




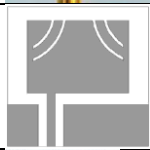
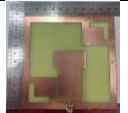

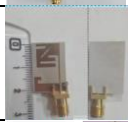
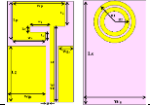
imaging applications [7]. For 5G, CPW-fed slot antennas with dual ground-plane slots enhance axial ratio and CP performance [8]. A compact asymmetric CPW-fed patch antenna with curved slits, designed on FR-4 substrate, achieves dual-band terahertz resonance at 0.813 THz and 1.254 THz with wide impedance bandwidths and high gain, making it suitable for 6G ultra-high-speed wireless communications [9]. Symmetrical L-shaped slits and widened tuning stubs enhance broadband CP operation [10]. Asymmetric ground planes and open slots improve mid/low-band AR and impedance matching [11]. Compact CPW-fed implantable antennas (2.45 GHz ISM band) use modified ground planes for wider bandwidth [12]. A miniaturized implantable CP antenna (3.4–7 GHz) is tested in human tissue [13]. CPW-fed inverted L-shaped monopoles with trimmed edges enhance IBW and ARBW [17]. Low-profile CP slot antennas cover multiple GNSS bands, with potential front-to-back ratio (FBR) improvement using reflectors [19]. Compact square-ring antennas with split corners achieve CP [20], while trapezoidal and L-shaped strips widen ARBW [21]. Triple-band CP antennas (2.4/3.5/5.8 GHz) use F-shaped feeds [22]. Transparent glass-substrate CP antennas maintain performance with mesh structures [23]. For ISM-band biotelemetry, CPW-fed antennas with etched slots ensure compact CP operation [24]. Narrowband microstrip patches on Polytetrafluoroethylene (PTFE)/ Flame Retardant Grade 4 (FR4) substrates suit 5.9 GHz DSRC [28]. Om-shaped [29] and U-shaped ground-plane antennas enable dual-band operation [31]. Square-shaped antennas with tunable stubs support multi-band applications [33]. The parametric analysis of incorporating stubs, slots, strips, and corner truncations, as discussed in [6] and summarized in Table 1, elucidates their collective impact on antenna performance.

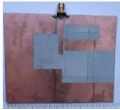
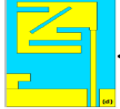
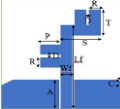
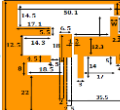



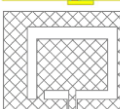
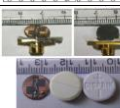



**Scientific Impact:** In CPW-fed antennas, integrating stubs, slots, strips, and corner cuts

offers powerful avenues to optimize electromagnetic behaviour:

- a) Stubs enable precise impedance matching, enhance bandwidth, and suppress harmonics, though at the cost of increased complexity.
- b) Slots in the radiator or ground plane facilitate antenna miniaturization, enable multi-band operation, enhance IBW, and allow polarization and pattern control, with minor trade-offs in radiation efficiency.
- c) Strips add tunable inductive or capacitive effects, improving impedance matching, coupling, and resonance tuning, while also assisting in multi-band and circular polarization performance.
- d) Corner cuts are crucial for generating circular polarization by exciting orthogonal modes with a 90° phase difference. They also influence impedance, and AR bandwidth, with slight gain reduction.

**Table 1.** Parametric effect of adding stubs, slots, strips, and cutting corners.

| Design Technique                | Antenna Layout  | Antenna Area (mm <sup>2</sup> ) | Di-electric Substrate Material ( $\epsilon_0$ ) | IBW (-10dB GHz) | Gain (dBi) | Applications                                       | Ref. |
|---------------------------------|---|---------------------------------|---|-----------------|------------|--|------|
| Stub with L-strip               |   | 18×18                           | FR4(4.4)  | 112%            | 4.2        | Broadband, Satellite Communications                | [2]  |
| Slotted Patch Array             |  | 270×200                         | Air (1)   | 32.3%           | 9.0        | Wi-Fi, WLAN  | [3]  |
| Slotted patch with DGS and stub |  | 30 × 30                         | FR4(4.4)  | 181%            | 9.4        | Microwave imaging (MI), SWB/UWB systems            | [7]  |
| Asymmetric CPW-fed curved slits |  | 0.5 × 0.5                       | FR4(4.4)  | 11.4%, 23.4%    | 6.1, 7.3   | 6G terahertz communications, high-speed data links | [9]  |
| Symmetrical Slits               |  | 116×116                         | FR4(4.4)  | 93.6%           | 3.4        | UHF RFID   | [10] |
| Asymmetric Ground               |  | 50×50                           | FR4(4.4)  | 103.5%          | 4.0        | WLAN, Wi-MAX                                       | [11] |
| Implanted Antenna               |  | 21×13.5                         | Rogers RT5880(2.2)                              | 47.7%           | 15.8       | ISM Band   | [12] |
| Miniaturized CP                 |  | 5×3                             | Polyimide substrate (2.78-3.48)                 | -               | 1.2        | ISM Band   | [13] |

|                        |   |         |                            |                           |                        |                                  |      |
|------------------------|---|---------|----------------------------|---------------------------|------------------------|----------------------------------|------|
| Rectangular Slots      |    | 88×89.9 | Rogers RO3006(6.5)         | 129.5%                    | 5                      | RFID, WLAN, Wi-MAX, GNSS         | [14] |
| Etched Slot Patch      |    | 21×13.5 | Flexible Roger RT5880(2.2) | 47.7%                     | -                      | ISM Band                         | [15] |
| Inverted L-shaped      |    | 25×25   | FR4(4.4)                   | 13.4%                     | 3.8                    | X- Band                          | [17] |
| Ground Slot, Reflector |    | 70×70   | Rogers RO3006(6.5)         | 28.4%                     | 3.6                    | GNSS                             | [19] |
| Split Corner Patch     |    | 54×54   | PVC (3-5)                  | 19.0%                     | 8-10                   | GNSS                             | [20] |
| L-shaped Strip         |    | 60×80   | FR4(4.4)                   | 100%                      | 3.7                    | Sub -6GHz                        | [21] |
| Triple-Band Feed       |    | 63.5×55 | -                          | -                         | 4.8                    | Wi-Fi, Wi-Max, WLAN              | [22] |
| Transparent CP         |   | -       | Glass (5-10)               | 28.6%                     | 3.9                    | GPS L1 Band                      | [23] |
| Slot Etched Patch      |  | 9.5×2.3 | Roger RT5880(2.2)          | 99.2%                     | 15                     | ISM Band                         | [24] |
| Narrowband Patch       |  | 15×24.5 | FR4(4.4)                   | -                         | 1.8                    | DSRC                             | [28] |
| Om-Shaped Patch        |  | 80×80   | FR4(4.4)                   | 2%,2.3%, 2.9%,2%          | 2.2, 1.8, 11, 9.4      | S-Band, IMT, C-Band, WI-MAX Band | [29] |
| Double Damru Shape     |  | 20×10   | FR4(4.4)                   | 1.1%,1.5, 1.4%,1.0%, 1.9% | 2.7,5.1, 5.3, 4.5, 8.7 | Ku Band, K-Band, 5G              | [30] |

## 2.2. Effect of Changes in the Substrate

**Material:** This approach examines various substrate materials and their key parameters, particularly focusing on dielectric properties, which critically influence the operational frequency range. A thicker substrate with a lower dielectric constant enhances radiation efficiency and widens the impedance bandwidth; however, it increases the antenna's physical dimensions. To address

this trade-off, high-permittivity substrates have been evaluated for Radio Frequency (RF) and microwave applications, enabling compact antenna designs while maintaining performance, as detailed in Table 2. The resonant frequency is determined by the substrate's area, thickness, and dielectric constant. Higher dielectric constants shift the fundamental resonance toward lower frequencies, especially when combined with

reduced substrate thickness. Consequently, high-permittivity materials facilitate antenna miniaturization without significantly compromising electrical performance [33].

**Scientific Impact:** The choice of substrate material in CPW-fed antennas plays a pivotal role in shaping electromagnetic performance, influencing parameters like miniaturization, bandwidth, efficiency, and fabrication ease. High-permittivity substrates such as Silicon, TMM 10i, and Duroid 6010 enable compact designs by lowering resonant frequencies, ideal for space-constrained RF/microwave systems, though often at the expense of radiation efficiency due to surface wave excitation. In contrast, low-permittivity

materials like Duroid 5880 and RO3700 deliver wider bandwidths and higher efficiency, trading off with larger physical sizes. Loss tangent is equally vital; low-loss substrates like Alumina and Duroid 5880 support high-gain and low-loss performance, while high-loss options like FR-4 degrade signal quality. From a manufacturing standpoint, soft substrates offer design flexibility but may introduce surface roughness and instability, whereas hard substrates ensure thermal durability and mechanical precision. Ultimately, achieving optimal antenna performance requires a careful balance of dielectric properties, mechanical traits, and application-specific needs.

**Table 2:** Properties of substrate materials

| Substrate                           | Dielectric Permittivity at 10 GHz | Loss Tangent at 10 GHz ( $10^4 \tan \delta$ ) | Surface Roughness ( $\mu\text{m}$ ) | Thermal Conductivity ( $\text{W/m}\cdot\text{K}$ ) | Dielectric Strength ( $\text{kV/cm}$ ) | Soft or Hard Substrate |
|-------------------------------------|-----------------------------------|---|-------------------------------------|--|--|------------------------|
| Alumina ( $\text{Al}_2\text{O}_3$ ) | 9.9                               | 1–2   | 0.05–0.25                           | 30–37  | 4000                                   | Hard                   |
| Aluminum Nitride (AlN)              | 8.9                               | 3–5   | 0.05–0.6                            | 150–170  | 150                                    | Hard                   |
| Glass (typical)                     | 4–7                               | 1   | 0.025                               | 0.8–1.2  | 350                                    | Hard                   |
| Silicon (Si)                        | 11.9                              | 10–100  | <0.001                              | 100–150  | 300                                    | Hard                   |
| Duroid 5880                         | 2.2                               | 12  | 0.8–1.0                             | 0.20   | 500                                    | Soft                   |
| Duroid 6002                         | 2.94                              | 12  | 0.8–1.0                             | 0.30   | 500                                    | Soft                   |
| Duroid 6010                         | 10.2–10.8                         | 27  | 0.8–1.0                             | 0.30   | 500                                    | Soft                   |
| Duroid R/flex 3700                  | 2.0                               | 20  | 0.8–1.0                             | 0.20   | 500                                    | Soft                   |
| Duroid RO3003                       | 3.0                               | 13  | 0.8–1.0                             | 0.50   | 500                                    | Soft                   |
| Duroid RO3006                       | 6.15                              | 25  | 0.8–1.0                             | 0.62   | 500                                    | Soft                   |
| Duroid RO3010                       | 10.2                              | 35  | 0.8–1.0                             | 0.62   | 500                                    | Soft                   |
| Duroid RO4003                       | 3.38                              | 27  | 0.8–1.0                             | 0.64   | 500                                    | Soft                   |
| Duroid RO4350B                      | 3.48                              | 40  | 0.8–1.0                             | 0.69   | 500                                    | Soft                   |
| TMM 6                               | 6.0                               | 23  | 0.8–1.0                             | 0.72   | 500                                    | Soft                   |
| TMM 10                              | 9.2                               | 22  | 0.8–1.0                             | 0.76   | 500                                    | Soft                   |
| TMM 10i                             | 9.8                               | 20  | 0.8–1.0                             | 0.76   | 1050                                   | Soft                   |



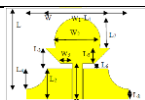
|      |         |     |    |      |         |      |
|------|---------|-----|----|------|---------|------|
| FR-4 | 4.5–4.8 | 220 | ~6 | 0.25 | 425–455 | Soft |
|------|---------|-----|----|------|---------|------|

**2.3. Effect of using defected ground structure (DGS):** A CPW-fed slot antenna incorporating a DGS is proposed [43] to improve gain for WLAN applications. The design employs vertical and horizontal DGS configurations, enhancing both gain and impedance bandwidth compared to conventional slot antennas. A dodecagram fractal broadband antenna is also presented, demonstrating multiband resonance, improved radiation patterns, and higher efficiency. The integration of DGS and feed slot further optimizes performance, suggesting potential refinements with alternative DGS geometries [51]. Another design features a tapered radiator with an embedded circular patch, operating at 4.45 GHz with reduced profile height. The DGS-implemented ground plane makes it suitable for wireless and biomedical devices [52]. Additionally, a T-shaped CPW-fed monopole antenna with staircase DGS achieves wide bandwidth, omnidirectional radiation, and stable gain, supporting Time Division-Synchronous Code Division Multiple Access (TD-SCDMA), Wideband Code Division

Multiple Access (WCDMA), LTE 33-41, Bluetooth, GPS, WLAN, and navigation systems [53]. Effects of using DGS parameters are summarized in Table 3.

**Scientific Impact:** Incorporating DGS into CPW-fed antennas offers a wealth of scientific benefits that elevate antenna performance. By introducing strategic defects in the ground plane, DGS enhances IBW, supporting wideband and UWB operations. It enables antenna miniaturization by increasing the electrical length without altering the physical size and serves as an effective harmonic suppressor, acting like a band-stop filter to eliminate unwanted frequencies. DGS also boosts radiation efficiency and gain by minimizing surface current losses, while offering superior control over current distribution, which aids in mode purity and polarization control, vital in circularly polarized and MIMO designs. Overall, DGS is a powerful technique for creating high-performance, compact, and adaptive CPW-fed antennas.

Table 3: Parametric effect of using defected ground structure

| Design Technique                                | Antenna Layout  | Antenna Area (mm <sup>2</sup> ) | Di-electric Substrate Material ( $\epsilon_0$ ) | IBW (-10dB GHz) | Gain (dBi) | Applications                          | Ref. |
|---|---|---------------------------------|---|-----------------|------------|---------------------------------------|------|
| Circular patch with rectangular slot-loaded DGS |  | 37 × 30                         | FR4(4.4)  | 90.9%           | 1.7–4.6    | 5G, C-band                            | [43] |
| Fractal DGS Patch                               |  | 23×24                           | FR4(4.4)  | 111.0%          | >1.5       | WiMAX, WLAN, FCC band, C- and X-band. | [51] |
| Tapered Radiator                                |  | 20×20                           | FR4(4.4)  | -               | 2.5        | UWB                                   | [52] |



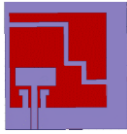


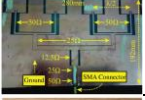

|                        |   |       |                  |       |     |  |      |
|------------------------|---|-------|------------------|-------|-----|--|------|
| Staircase DGS Monopole |  | 82×82 | RT-Duroid (2.33) | 84.0% | 6.4 | WLAN, CDMA, GPS, Wifi, Bluetooth, LTE. | [53] |
|------------------------|---|-------|------------------|-------|-----|--|------|

Table 4: Parameters show the effect of using arrays

| Design Technique        | Antenna Layout  | Antenna Area (mm <sup>2</sup> ) | Di-electric Substrate Material ( $\epsilon_0$ ) | IBW (-10dB GHz) | Gain (dBi) | Applications                            | Ref. |
|-------------------------|---|---------------------------------|---|-----------------|------------|---|------|
| CPW-fed Array           |  | -                               | FR4 (4.4)                                       | 6.0%            | 12.4       | Aerospace                               | [36] |
| Wideband 2×2 CP Array   |  | 170×170                         | FR4 (4.4)                                       | 67.0%           | 6.0        | UWB                                     | [54] |
| Flexible CP Patch Array |  | 280×192                         | (PET) substrate (1.8)                           | -               | 10.0       | ISM                                     | [55] |
| 1×2 Array with DGS      |  | 170×105                         | Plexiglass substrate                            | 20.0%, 74.0%    | 6.3        | GPS, GSM, LTE, Bluetooth, Wi-Max, UTMS. | [35] |

#### 2.4. Effects of using arrays in radiation patch:

A compact CPW-slot line-fed CP microstrip array [36] demonstrates improved performance with a high front-to-back ratio. The design features simple geometries, low profile ( $0.02\lambda_0$ ), and lightweight construction, achieving significant impedance bandwidth and 4.10% CP bandwidth while maintaining adequate gain. An alternative wideband CP array [54] employs sequential rotation feeding, showing enhanced performance in array configuration with better gain across the operational band and stable radiation characteristics. For biomedical applications, a flexible PET-based CPW-fed 2×2 patch array operates at 2.68 GHz with 10 dBi peak gain. The cost-effective design uses adhesive copper foils instead of traditional conductive inks, demonstrating good conformal performance and potential for wearable systems. Further optimization for ISM band applications is planned [55]. The designed 1×2 antenna array utilizes a Plexiglas substrate with defected ground structure


(DGS) implementation for enhanced bandwidth and impedance matching. The dual-band operation covers: 1.08-1.32 GHz (GPS band), 1.7-3.7 GHz (encompassing GSM, UMTS, Bluetooth, LTE, and WiMAX applications). A comprehensive parametric analysis of the DGS-modified ground plane revealed significant bandwidth improvement. The array demonstrates optimal radiation characteristics, including high efficiency and peak gain performance [35]. Key radiation patch array effects are summarized in Table 4.

**Scientific Impact:** Using arrays in the radiation patch of CPW-fed antennas enables a highly efficient, multi-functional, and application-tailored antenna design strategy. Scientific benefits include enhanced gain, wider bandwidth, CP improvement, and pattern control, making them suitable for advanced systems in aerospace, UWB, wearable tech, biomedical devices, and multiband wireless communications. When

combined with techniques like DGS and flexible substrates, these arrays offer next-

generation solutions for compact and high-performance antennas.

**Table 5:** Parameters showing the effect of using defected substrate

| Design Technique         | Antenna Layout  | Antenna Area (mm <sup>2</sup> ) | Di-electric Substrate Material ( $\epsilon_0$ ) | IBW (-10dB GHz) | Gain (dBi) | Applications | Ref. |
|--------------------------|---|---------------------------------|---|-----------------|------------|--------------|------|
| Defected Substrate Patch |  | 42×36                           | FR4 (4.4)                                       | 100.0%          | 6.0        | C and X Band | [37] |

**2.5. Effect of using defected substrate:** A CPW-fed defected substrate microstrip antenna is proposed for wideband applications. Defected substrates also reduce the size of an antenna. The radiating patch of the proposed antenna is in the form of an extended U-shape. The space around the radiator is utilized by extending the ground plane on both sides of the radiator. The antenna has good return loss, constant group delay, and good radiation characteristics within the entire operating band. It has a maximum value of 88% and is applicable for C and X band applications [37]. Here is the effect of using defected substrate in Table 5.

**Scientific Impact:** Defected substrates offer a unique way to engineer antenna performance beyond traditional geometry tuning. By strategically modifying the substrate, designers can achieve miniaturization, wider bandwidth, higher efficiency, and better thermal stability.

**2.6. Effect of using Notch band characteristics:** A rectangular radiating patch is optimized to achieve an UWB response with an enhanced VSWR bandwidth of 11.88 GHz, while incorporating band-notched functionality at 3.5 GHz WiMAX without compromising radiation performance. Simulation results confirm its suitability for UWB applications with selective frequency rejection [25]. Further, compact CPW-fed UWB monopole



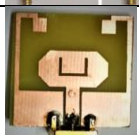

antennas are proposed, utilizing split ring slots (SRSs) for band-notched characteristics. The modified rectangular patch ensures wide impedance bandwidth across the UWB spectrum, while integrated SRS elements introduce rejection bands at 5.3 GHz WLAN and 7.4 GHz (X-band satellite communication). These designs are fabricated on low-cost FR4 substrates, maintaining a compact form factor [49]. The antenna uses a CPW feed, U-slot, split-ring resonators (SRRs), and mushroom-type EBG structures to achieve sharp notch characteristics [58]. Additionally, a CPW-fed UWB antenna with an inverted L-shaped structure demonstrates WLAN band rejection (5.15–5.85 GHz) while covering 3.02–11.34 GHz. Simulations align well with measurements, validating its performance [59]. The impact of notch band integration on antenna performance is summarized in Table 6.

**Scientific Impact:** Notch band integration in CPW-fed UWB antennas enables highly selective frequency rejection without compromising bandwidth, gain, or radiation performance. Using techniques like U-slots, SRRs, SRSs, and EBGs, designers can tailor the antenna response to suppress unwanted signals from coexisting services, making these antennas highly suitable for UWB communication, radar, and interference-prone environments. Combined with compact size, low-cost fabrication, and high

efficiency, these antennas represent a scientifically robust and practically viable

solution for next-generation wireless systems.

**Table 6:** Parameters showing the effect of using Notch band characteristics

| Design Technique       | Antenna Layout  | Antenna Area (mm <sup>2</sup> ) | Di-electric Substrate Material ( $\epsilon_0$ ) | IBW (-10dB GHz) | Gain (dBi) | Applications                                     | Ref. |
|------------------------|---|---------------------------------|---|-----------------|------------|--|------|
| U-slot, SRRs, EBGs     |  | 27×27                           | FR4(4.4)  | 147.0%          | 3.6-8.2    | Wi-MAX, WLAN, X-Band                             | [25] |
| Split Ring Slot (SRS)  |  | 18×18                           | FR4(4.4)  |                 | 8.8        | UWB  | [49] |
| U-slot, SRRs, and EBGs |  | 25 × 25                         | FR4(4.4)  | 127.4%          | 1.2–3.9    | UWB systems, interference rejection for C/X-band | [58] |
| Inverted L-slot        |  | 25×25                           | FR4(4.4)  | 47.4%, 58.6%    | 3          | UWB  | [59] |

**2.7. Effects of using metamaterial substrate:** Digital light processing (DLP) and the micro-dispensing procedure for Rogers Radix<sup>TM</sup> and Nova Centrix HPS-FG57B conductive paste, respectively [18], are used in this work to additionally build the CPW-back-fed meta surface patch antenna. For wideband and polarization control, the meta surface is made up of truncated patches with designed sizes and relative arrangements. By using Rogers Radix, the substrate thickness could be optimized to achieve improved axial ratio, gain, and impedance bandwidth. For use with CubeSat applications, a wideband CP-printed dipole antenna with AMC is suggested [16]. Placing AMC at the back of the antennas improves the gain of the suggested antenna. The design includes a triangular cut at the upper edge of the right ground plane and asymmetric ground planes to achieve CP. The suggested printed monopole antenna has a wider 3dB ARBW and a greater gain while taking up less space in terms of physical dimensions. A metamaterial super-substrate-loaded concentric circle-shaped antenna with a coplanar waveguide [44] has been studied for

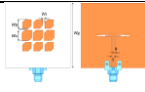
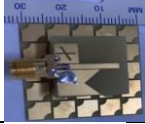
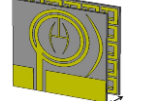

gain enhancement in three wideband modes. The proposed meta-surface's near-zero refractive index increases gain over a wide range of operations. It is more efficient and can be used for various applications, such as satellite communication, military, and medical monitoring. A resonator-based 3x3 metamaterial array [46] is used as a reflector plane below a wideband antenna to obtain optimal bandwidth and gain features. The antenna displays better outcomes and can be utilized in various satellite, wearable, and wireless applications. The proposed antenna has 2 to 16 GHz of total bandwidth and a peak gain of 13.1 dB. Table 7 shows the effect of using a metamaterial substrate.

**Scientific Impact:** The incorporation of metamaterial substrates in CPW-fed antennas enables a paradigm shift in antenna design, achieving high gain, ultra-wide bandwidth, polarization control, and compact, low-profile construction. With applications spanning CubeSats, X-band, WLAN, LTE-A, Wi-Fi, 5G, and UWB systems, MTM-enhanced antennas provide next-generation performance critical for advanced wireless, aerospace, and biomedical platforms. The

combination of engineered electromagnetic properties with innovative fabrication methods like DLP and additive printing

further strengthens their practical and scientific value.

**Table 7:** Parameters showing the effect of using a metamaterial substrate.

| Design Technique            | Antenna Layout  | Antenna Area (mm <sup>2</sup> ) | Di-electric Substrate Material ( $\epsilon_0$ ) | IBW (-10dB GHz) | Gain (dBi) | Applications                       | Ref. |
|-----------------------------|---|---------------------------------|---|-----------------|------------|------------------------------------|------|
| Additively Manufactured MTS |  | 48.6×48.6                       | RogersRadix, NovaCentrix HPS-FG57B              | 63%             | 7.7        | X-Band                             | [18] |
| CP Printed Dipole + AMC     |  | 6.2×6.2                         | FR4(4.4)  | 97.5%           | 7.3        | X-Band, CubeSat                    | [16] |
| Concentric Circle + MTM     |  | 28×28                           | FR4(4.6)  | 42%, 22%, 47.5% | 6.2        | WLAN, LTE-A, 5G, Wi-Fi, and X-band | [44] |
| MTM Reflector (3×3 Unit)    |  | 14.8×14.8                       | FR4(4.4)  | 155%            | 13.1       | UWB                                | [46] |

**2.8. Effects of using the frequency-selective surface technique in CPW:** A novel miniaturized frequency-selective surface (FSS) design [34] is presented for CPW antenna gain enhancement, demonstrating a gain improvement from 1.8 dBi to 2.6 dBi while maintaining omnidirectional radiation. Optimal performance occurs at 2.45 GHz with scalable gain through FSS element multiplication, making it suitable for IoT, ground-penetrating radar, wireless communications, and medical imaging applications. A compact UWB antenna system incorporating a hexagonal patch with multiple stubs (5-17 GHz bandwidth) and a 5×5-unit cell FSS layer (9 mm spacing) achieves 15 GHz ultrawideband operation (3-18 GHz). This configuration demonstrates exceptional potential for 5G/6G applications due to its optimized size-volume-bandwidth-gain characteristics [39]. An aperture-coupled printed antenna [56] with dual-layer FSS reflectors (7×5 crossed elements) shows significant performance improvements: 63% bandwidth enhancement and 29.4%/15.8%

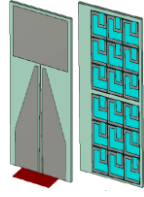


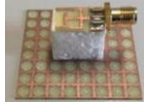
gain increase compared to single-layer implementations. The compact design features a bottom-substrate feed antenna and miniaturized unit cells, making it ideal for long-range communications. For UWB applications, a 50% miniaturized monopole antenna with 8×8 FSS reflector array achieves 2.55-13 GHz bandwidth (extended to 2.61-13 GHz with FSS) and stable 8.6 dBi peak gain. Experimental validation confirms  $\geq 4$  dBi gain improvement and enhanced lower-frequency bandwidth performance [57]. Table 8 summarizes the performance enhancements achieved through FSS integration in CPW antennas.

**Scientific Impact:** FSS integration transforms CPW-fed antennas into high-performance systems by combining filtering, gain enhancement, and bandwidth extension in a single compact structure. The choice of FSS geometry (crossed dipoles, hexagons, CSRRs) and layer configuration (single vs. dual) depends on the target frequency, gain, and application requirements. Through effective integration with stubs, patches, or

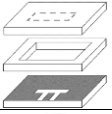
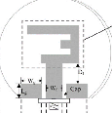
layered architectures, FSS transforms traditional CPW antennas into high-

performance, frequency-agile systems ready for modern wireless challenges.

**Table 8:** Parameters showing the effect of using a frequency-selective surface (FSS)

| Design Technique  | Antenna Layout   | Antenna Area (mm <sup>2</sup> ) | Di-electric Substrate Material ( $\epsilon_0$ )                        | IBW (-10dB GHz) | Gain (dBi) | Applications        | Ref. |
|-------------------|--|---------------------------------|--|-----------------|------------|---------------------|------|
| Miniaturized FSS  |   | 28.8×46.5                       | Upper substrate FR4(4.6)<br>Lower substrate Rogers RT/duroid 5880(2.2) | 62.5%           | 1.8-2.6    | IoT                 | [34] |
| Stub-loaded Patch |   | 50×50                           | Rogers RT/duroid 6002(2.94)  | 109%            | 10.5       | UWB                 | [39] |
| Dual-layer FSS    |   | 30×32                           | FR4(4.4)   | 82.3%,44.5%     | 8.4        | Long Distance Comm. | [56] |
| UWB FSS Reflector |  | 40×40                           | FR4(4.4)   | 134%            | 8.6        | UWB                 | [57] |

**Table 9:** Parameters showing the effect of high permittivity substrates

| Design Technique                     | Antenna Layout  | Antenna Area (mm <sup>2</sup> ) | Di-electric Substrate Material ( $\epsilon_0$ )  | IBW (-10dB GHz) | Gain (dBi) | Applications                         | Ref. |
|--------------------------------------|---|---------------------------------|--|-----------------|------------|--------------------------------------|------|
| High- $\epsilon_r$ Microstrip Design |  | -                               | Taconic CER-10   | -               | 6.1        | 24GHz                                | [48] |
| Inverted E-shape Monopole            |  | 490                             | (Mg <sub>0.93</sub> Zn <sub>0.07</sub> ) <sub>2</sub> SnO <sub>4</sub> microwave ceramic Substrate (8.5) | 33.1%, 27.3%    | 4.4        | ISM, HIPERLAN, UNII and WiMAX bands. | [50] |

**2.9. Effect of using high permittivity substrates:** Two designs [48] of 24 GHz microstrip patch antennas using high-dielectric constant substrates have been presented, with high gain achieved using micromachining and superstrate. Multilayer construction and coplanar waveguides are used, with an air gap introduced to avoid surface waves. The new design uses the superstrate effect, and the measured gain value exceeds 6 dBi. Simulation and

measurement results are presented for two designs on high-permittivity substrates. A compact CPW-fed inverted-E-shaped monopole was successfully fabricated on a high-permittivity substrate. The antenna has a 10dB return loss and covers the ISM, Unlicensed National Information Infrastructure (UNII), High Performance Radio Local Area Network (HIPERLAN), and WiMAX bands. The monopole has a smaller size and comparable bandwidth

compared to the literature [50]. The effect of using high-permittivity substrates is shown in Table 9.

**Scientific Impact:** Using high-permittivity substrates in CPW-fed antennas facilitates size reduction, resonant frequency control, and gain enhancement, making them well-suited for compact, high-frequency, and multi-band applications. Through design techniques like micromachining, superstrate addition, and air-gap optimization, the traditional limitations of high- $\epsilon_r$  materials (e.g., bandwidth narrowing or surface wave excitation) can be effectively mitigated, allowing engineers to harness their full potential in ISM, 5G, satellite, and millimeter-wave systems.

**2.10. Effects of using Conductor-backed CB-CPW antennas:** A novel broadband monopole antenna design [41] has been engineered to achieve enhanced bandwidth characteristics while maintaining a compact form factor. The optimized structure demonstrates superior performance metrics including: High return loss ( $>15$  dB), Extended operational bandwidth (covering ISM, RFID, and WLAN bands), Radiation efficiency exceeding 85%, Excellent thermal management properties. The design incorporates cost-effective manufacturing processes while offering: Minimal radiation losses ( $<0.5$  dB), Robust mechanical durability, Aesthetic structural integrity, Simplified assembly procedures. A CPW (CB-CPW) broadband antenna design [42] has been developed for multi-beam operation in WLAN (5.15-5.25 GHz), RFID (5.8 GHz), and WiMAX applications. The innovative configuration features semi-circular ground

plane topology, Parasitic ground elements, Triple CPW feed structure. This architecture achieves broadband impedance matching ( $VSWR < 2:1$ ), Enhanced thermal dissipation, Mechanical robustness. Experimental validation through prototype fabrication confirms the simulated performance characteristics. Table 10 quantitatively compares the performance enhancements achieved through CB-CPW implementation. P.S. Kumar et al [45] have proposed a miniaturized three-band antenna with a backed MTS. The triple frequency is created by combining the diamond-shaped patch with the (CB-MTS) CPW-fed antenna. The antenna covers the following 5G bands: 2.4–2.484 GHz for the IoT 3.6–4.2 GHz for the 5G mobile phone for satellite communication applications 5.35–5.47 GHz for the future of mobile broadband applications The proposed antenna has a 72.7% size reduction compared to a conventional rectangular patch. Table 10. shows the effect of using (CB-MTS) CPW antennas.

**Scientific Impact:** Using conductor-backed (CB) structures in CPW-fed antennas enables broadband operation, footprint reduction, thermal resilience, and high radiation efficiency. The combination of electromagnetic optimization and mechanical benefits makes CB-CPW antennas highly suitable for compact, low-cost, and high-performance wireless systems, including 5G, WLAN, RFID, IoT, and CubeSat platforms. Designs like CB-MTS further extend these advantages by adding multiband functionality and metasurface-enhanced gain, paving the way for next-generation miniaturized RF devices.

**Table 10:** Parameters showing the effect of using conductor-backed CB-CPW antennas

| Design Technique | Antenna Layout | Antenna Area (mm <sup>2</sup> ) | Di-electric Substrate Material ( $\epsilon_0$ ) | IBW (-10dB GHz) | Gain (dBi) | Applications | Ref. |
|------------------|----------------|---------------------------------|---|-----------------|------------|--------------|------|
|------------------|----------------|---------------------------------|---|-----------------|------------|--------------|------|



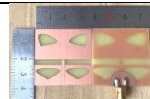

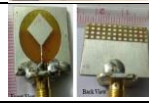
|                       |   |       |          |                   |     |                    |      |
|-----------------------|---|-------|----------|-------------------|-----|--------------------|------|
| CB-CPW Monopole       |  | 38×38 | FR4(4.4) | 60%               | 3.3 | ISM, RFID, WLAN    | [41] |
| Triple CPW Feed Patch |  | 40×40 | FR4(4.4) | 60%               | 3.9 | WLAN, RFID, Wi-Max | [42] |
| CB-MTS Patch Antenna  |  | 22×23 | FR4(4.4) | 7.5%, 13.2%, 7.4% | 3.6 | 5G                 | [45] |

Table 11: Parameters showing the effect of using MGS, FSS, DGS, and MTM.


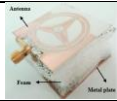

| Design Technique      | Antenna Layout  | Antenna Area (mm <sup>2</sup> ) | Di-electric Substrate Material ( $\epsilon_0$ ) | IBW (-10db GHz)          | Gain (dBi) | Applications              | Ref. |
|-----------------------|---|---------------------------------|---|--------------------------|------------|---------------------------|------|
| MGS + FSS + DGS + MTM |  | 17×20                           | FR4(4.4)  | 35.6%, 18%, 10.7%, 18.3% | --         | GSM, Wi-Fi, WLAN, Wi-Max, | [32] |

Table 12: Parameters showing the effect of using metal reflector plates.

| Design Technique                          | Antenna Layout  | Antenna Area (mm <sup>2</sup> ) | Di-electric Substrate Material ( $\epsilon_0$ ) | IBW (-10db GHz)    | Gain (dBi) | Applications                 | Ref. |
|---|---|---------------------------------|---|--------------------|------------|------------------------------|------|
| CPW-fed patch with reflector              |  | 35×35                           | Rogers 4003C (3.55)                             | 15.1%              | 7.3        | WBAN                         | [27] |
| Notch-banded CPW-fed patch with reflector |  | 30×20                           | FR4(4.4)  | 11.0%, 4.3%, 43.4% | 10.0       | Bluetooth, WLAN, WI-MAX, UWB | [40] |

**2.11. Effect of using Modified Ground Structure (MGS) and Frequency Shifting Strips (FSS), along with Defected Ground Structure (DGS) and Metamaterial (MTM):** An FR4-based CPW-fed multiband antenna with a 17×20mm diameter is designed with a modified ground structure, frequency shifting strip, defected ground structure, and metamaterial loading on the lower side of the antenna. This multiband antenna operates at 1.702 MHz, 3.202 MHz, 5.302 MHz, and 10.302 MHz, covering GSM 1800/900 MHz, Wi-Fi/WLAN (5.2/5.5 GHz), and WiMAX 3.3 GHz [32]. Table 13 shows

the effects of using MGS, FSS, DGS, and MTM.

**Scientific Impact:** Using MGS, FSS, DGS, and MTM in CPW-fed antennas results in a powerful compact, multiband, and broadband solution with controlled radiation and harmonic suppression. These techniques synergize to improve impedance bandwidth, enable multiband tuning, reduce antenna size, and optimize radiation characteristics, making them ideal for multi-standard wireless devices, including GSM, Wi-Fi, WLAN, and WiMAX. The compact design with frequency agility also ensures high

integration potential in portable, wearable, and smart IoT platforms.

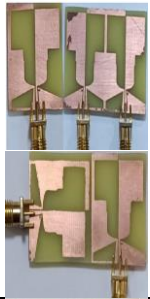


### 2.12. Effect of using metal reflector plates:

Mercedes-Benz has developed a modified logo with a CPW-fed antenna to control radiation towards the human body. A metal plate was used as a reflector to reduce human body loading on the antenna. The antenna performed well on the actual and modeled body and is suitable for WBAN communication systems [27]. Table 14. shows the effect of using metal reflector plates. K.G. Jangid et al [40] have described the design and performance of a UWB antenna with triple band notched features and increased gain. The proposed CPW-fed patch antenna has two U-shaped slots on the patch, an inverted U-shaped slot in the feed line, and a metallic reflector beneath the antenna structure. The three rejection bands were obtained by inserting three U-slots of varying sizes and locations into the radiator. The

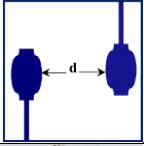
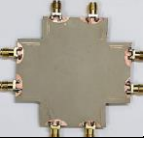
antenna's maximum gain is close to 9.88 dBi at 7.4 GHz. This antenna is helpful for modern ultra-wideband communication systems, except for 3.5 GHz WIMAX, IEEE 802.11a/h/j/n WLAN, and ITU 8 GHz systems. Table 12 shows the effect of using metal reflector plates with notch bands.

**Scientific Impact:** Metal reflector plates in CPW-fed antennas significantly enhance performance by reducing SAR and enhancing safety in wearable devices, improving gain and directionality, enabling notch-band rejection for interference avoidance, and stabilizing radiation patterns in wideband and multi-band scenarios. This makes them highly effective for WBAN, Bluetooth, WLAN, WiMAX, and UWB applications, particularly where directional control and spectral cleanliness are essential.

**Table 13:** Parameters show the effect of using CPW-fed MIMO Antennas

| Design Technique  | Antenna Layout  | Antenna Area (mm <sup>2</sup> ) | Di-electric Substrate Material ( $\epsilon_0$ ) | IBW (-10db GHz) | Gain (dBi) | Applications                | Ref. |
|---|---|---------------------------------|---|-----------------|------------|-----------------------------|------|
| Modified F-shaped radiator<br>Spatial Diversity,<br>Pattern Diversity<br>MIMO |  | 24×22 (Single Element)          | FR4(4.4)  | 173.3%          | 8.6        | UWB, SWB                    | [38] |
|   |   | 24×43 (Spatial Diversity)       | FR4(4.4)  | 174.2%          |            |                             |      |
|   |   | 24×47 (Pattern Diversity)       | FR4(4.4)  | 174.2%          |            |                             |      |
| Octagonal slot, L-shaped stub, two element MIMO                               |  | 38.4×20                         | FR4(4.4)  | 154.3%          | 8.9        | 5G, C-Band, K-Band, mm Wave | [26] |
| Hexagonal shaped patch, L-shaped grounded strips                              |  | 40×40                           | Polyimide (3.5)                                 | 122.5%          | 6.3        | UWB and X-Band Applications | [60] |



|   |   |               |              |        |     |                         |      |
|---|---|---------------|--------------|--------|-----|-------------------------|------|
| Modified rectangular radiating element. |  | 6×17.37       | RO5880 (2.2) | 15.1%  | 6.7 | 5G mm-wave applications | [61] |
| Key-type slotted-radiating patch        |  | 126.49×126.49 | RO5880 (2.2) | 165.7% | 9.9 | Multi-band applications | [62] |

### 2.13. Effects of using MIMO CPW-fed antennas:

A quad-band circularly polarized monopole antenna [38] is presented for extended UWB applications, with a two-element MIMO configuration optimized for C-band, K-band, and mm-wave operation. Key performance characteristics include Peak gain of 6.73 dB, Radiation efficiency of 96%, impedance bandwidth of 3.7-29.27 GHz, four distinct CP bands with 3 dB axial ratio bandwidths of 35.5%, 1.5%, 4.6%, and 0.51%. The design incorporates modified U-shaped symmetrical decoupling structures in the MIMO configuration, achieving port isolation >16 dB across the operational bandwidth, suitable for C-band, Ku-band, 5G, Ka-band, mm-wave, and UWB applications [26]. A complementary quasi-complementary super-wideband antenna element (24 × 22 mm) demonstrates ultra-wide bandwidth of 3-42.1 GHz (173.3% fractional bandwidth), Modified F-shaped radiator with tapered CPW feed, Ground plane slot optimization, MIMO configuration (24 × 43 mm) maintains port isolation ≥15 dB, envelope correlation coefficient <0.008, operational range: 2.9-42.14 GHz [38]. This paper presents a compact 4-port CPW-fed flexible MIMO antenna, where the elements are arranged orthogonally to enhance isolation (> -17 dB) without additional decoupling structures. It demonstrates excellent diversity performance and stable operation under bending, making it ideal for wearable electronics [60]. This work proposes a two-port MIMO antenna with anti-parallel layout and defected ground structure (DGS) for mmWave 5G applications. The design eliminates the need for complex decoupling techniques and

ensures robust diversity performance [61]. This paper introduces an eight-port key-shaped MIMO antenna with an asymmetric feedline. The antenna exhibits stable performance under 45° bending and is well-suited for multi-band wireless systems [62]. Table 13 quantifies the performance enhancements achieved through CPW-fed MIMO antenna implementation.

**Scientific Impact:** MIMO integration in CPW-fed antennas transforms them into high-performance systems with ultra-wideband coverage, low mutual coupling & high isolation, enhanced gain and efficiency, compact and flexible configurations, suitability for UWB, 5G, mmWave, and wearable applications. These scientific enhancements make CPW-fed MIMO antennas indispensable in next-gen wireless platforms requiring speed, reliability, compactness, and multi-band diversity.

**3. Comparative Outcomes:** In this article, we review the various design techniques of CPW-fed antennas. Adding the stubs, slots, and strips method has miniaturized the size of the antenna for multi-band wireless applications [7,9]. The microwave soft substrate materials for microwave applications are usually used for CPW-fed patch antenna designs with different permittivities and thicknesses [12]. The thicker substrate offers more efficiency and a wider IBW for a lower dielectric constant, but a larger antenna. Hence, substrates with high dielectric constants favor small antenna sizes as compared to other conventional antennas [48, 49]. DGS offers significant gain

improvement over the entire band of operation compared to conventional slot antennas without DGS [53]. The number of arrays on the radiating patch also improves the gain of the antenna. [36, 55]. Using arrays with the DGS technique contributed to the bandwidth enhancement of the antenna with good efficiency and gain [35]. CPW-fed defected substrate microstrip antennas show a reduction in antenna size with wideband applications [37]. CPW-fed antennas with band-notch characteristics are used to enhance impedance bandwidth for the entire UWB frequency range and to generate band rejection at desired frequencies [25, 49]. Metamaterial arrays can be used as a reflector plane below the ground structure to obtain optimal bandwidth and gain features for UWB applications [46]. By using an FSS array containing subsequent unit cells, it improves the gain and bandwidth over the entire frequency range and is also offered for antenna miniaturization [39, 56, 57]. The CB-CPW band monopole antenna has been developed with various features to expand bandwidth and reduce size, be easy to process and assemble, have fast heat-dissipating speed, and have small radiation [41, 42].

#### 4. Conclusion and Future Directions

**(a) Research Contributions:** This study comprehensively analyzes the impact of various design techniques like stubs, slots, DGS, FSS, metamaterials, and substrate modifications on CPW-fed antenna performance. Key contributions include:

1. **Bandwidth Enhancement:** Techniques like DGS and asymmetric ground planes achieve 181% IBW [7] and multi-band operation [6].
2. **Circular Polarization (CP):** L-shaped strips and corner truncations improve ARBW [10, 21].
3. **Miniaturization:** High-permittivity substrates (e.g., RO3010) and defected structures reduce size while maintaining performance [37, 48].

4. **Interference Mitigation:** Notch bands (e.g. U-slots, SRRs [58]) reject WLAN/WiMAX frequencies without compromising UWB operation.

5. **Gain and Efficiency:** Metamaterial substrates [16] and FSS reflectors [34] boost gain up to 13.1 dBi.

#### (b) 5G and Beyond Applications

1. **Sub-6 GHz and mm Wave:** Compact designs [26, 61] support 5G bands (3.5 GHz, 28 GHz) with MIMO configurations.
2. **6G Terahertz:** Curved-slit antennas [9] enable dual-band THz operation (0.813/1.254 THz) for ultra-high-speed communications.
3. **IoT/Wearables:** Flexible arrays [55] and implantable antennas [12] cater to biomedical and conformal applications.

#### (c) Research Gaps and Future Directions

1. **Reconfigurability:** Limited work on tunable notch bands using varactors/MEMS for dynamic spectrum adaptation.
2. **AI-Driven Design:** Machine learning could optimize stub/slot placement for enhanced CP and bandwidth.
3. **Energy Efficiency:** Integration with RF energy harvesting for self-powered IoT devices.
4. **THz and Optical Antennas:** Further exploration of transparent antennas [23] and plasmonic structures for 6G.
5. **MIMO Scalability:** Decoupling techniques for high-density MIMO arrays in mm Wave systems.

#### Motivation and Outlook

The demand for compact, multi-band, and high-gain antennas drives innovation in CPW-fed designs. Future work should focus on:

1. **Multi-functional Integration:** Combining sensing, energy harvesting, and communication in a single antenna.

2. **Sustainable Materials:** Eco-friendly substrates with low loss for green wireless systems.
3. **Standardization:** Benchmarking performance metrics for 5G/6G and industrial IoT applications.

This study bridges theoretical advancements with practical applications, paving the way for next-generation wireless systems.

**Conflict of Interest:** The Authors declare no conflicts of interest.

**Acknowledgment:** The authors gratefully acknowledge the unwavering support and encouragement provided by the Department of EECE, Sharda University, which has been instrumental in the successful completion of this research.

## 5. References:

- [1] Z.-H. Ma et al., Design of planar microstrip Ultrawideband circularly polarized antenna loaded by annular-ring slot, *International Journal of Antennas and Propagation*, 2021, pp. 1–10.
- [2] S. Patil, A.K. Pandey, and V.K. Pandey, A compact, wideband, dual polarized CPW-fed asymmetric slot antenna for wireless systems, *Journal of Microwaves, Optoelectronics and Electromagnetic Applications*, 19(3), 2020, pp. 343–355.
- [3] K.L. Chung et al., Circularly-polarized linear antenna array of non-identical radiating patch elements for WIFI/WLAN applications, *AEU - International Journal of Electronics and Communications*, 129, 2021, p. 153526.
- [4] U. Ullah and S. Koziel, A geometrically simple compact wideband circularly polarized antenna, *IEEE Antennas and Wireless Propagation Letters*, 18(6), 2019, pp. 1179–1183.
- [5] S.K. Singh, T. Sharan, and A.K. Singh, Enhancing the axial ratio bandwidth of circularly polarized open ground slot CPW-fed antenna for Multiband Wireless Communications, *Engineered Science*, 2021.
- [6] M. Kumar, Y. D. Banda, F. W. Aldbea, S. V. Savilov, S. K. Singh et al., Investigation of substrate materials laminated CPW-Fed patch antennas: Opportunities and challenges, *CNS&E Journal*, 1(3), May 2024, pp. 211–220.
- [7] M. Sekhar, N. Suman et al., CPW Fed Super-Wideband Antenna for Microwave Imaging Application, *Progress in Electromagnetics Research C*, 130, 2023, 201–212.
- [8] S.F. Seyyedrezaei et al., A novel small size CPW-fed slot antenna with circular polarization for 5G application, *Progress in Electromagnetics Research C*, 106, 2020, pp. 229–238.
- [9] K. K. Naik et al., Asymmetric CPW-fed patch antenna with slits at terahertz applications for 6G wireless communications, *Wireless Networks*, 30(6), 2024, 2343–2351.
- [10] R. Ma and Q. Feng, Design of broadband circularly polarized square slot antenna for UHF RFID applications, *Progress in Electromagnetics Research C*, 111, 2021, pp. 97–108.
- [11] Q. Fu, Q. Feng and H. Chen, Design and optimization of CPW-fed broadband circularly polarized antenna for multiple communication systems, *Progress in Electromagnetics Research Letters*, 99, 2021, 65–74.
- [12] A.D. Butt et al., Single-fed broadband CPW-fed circularly polarized implantable antenna for sensing medical applications, *PLOS ONE*, 18(4), 2023.
- [13] S. Ahmad et al., A compact wideband flexible circularly polarized

- implantable antenna for biotelemetry applications, 2021 IEEE International Symposium on Antennas and Propagation and USNC-URSI Radio Science Meeting (APS/URSI), 2021.
- [14] A. Gharaati et al., A low-profile wideband circularly polarized CPW slot antenna, *AEU - International Journal of Electronics and Communications*, 129, 2021, 153534.
- [15] S. Ahmad et al., A low-profile CPW-fed circularly polarized antenna for biomedical applications, 2022 IEEE International Symposium on Antennas and Propagation and USNC-URSI Radio Science Meeting (AP-S/URSI), 2022.
- [16] M.E. Hammoumi et al., A wideband circularly polarized CPW-fed printed monopole X-band antenna for CubeSat Applications, *IEEE Access*, 11, 2023, 121077–121086.
- [17] R. Tripathy, K. Sumana, and S.R. Patre, A low-profile UNIPLANAR circularly polarized monopole antenna for X-band applications, 2022 IEEE 9th Uttar Pradesh Section International Conference on Electrical, Electronics and Computer Engineering (UPCON), 2022.
- [18] J. O’Keefe et al., An additively manufactured CPW-back-fed wideband circularly-polarized radix metasurface patch antenna for X-band space applications, 2023 IEEE International Conference on Wireless for Space and Extreme Environments (WiSEE), 2023.
- [19] A. Gharaati, A. Goudarzi, and R. Mirzavand, compact circularly polarized CPW-fed antenna for GNSS applications, 2021 IEEE International Symposium on Antennas and Propagation and USNC-URSI Radio Science Meeting (APS/URSI), 2021.
- [20] A. Nikam and R. Patil, Design of circularly polarized antenna for vehicular GNSS application, 2023 Second International Conference on Electrical, Electronics, Information and Communication Technologies (ICEEICT), 2023.
- [21] B. Qiu and Y. Li, Asymmetric CPW-fed wideband circularly polarized antenna for sub-6 GHz application, 2020 IEEE 3rd International Conference on Electronic Information and Communication Technology (ICEICT), 2020.
- [22] N. K. et al., Time variant circularly polarized CPW antenna for WIFI/ISM/wi-max/wi-lan communication applications, 2023 IEEE Wireless Antenna and Microwave Symposium (WAMS), 2023.
- [23] W. Zhong and Y.-X. Sun, Wideband circularly polarized antenna on glass substrate with high optical transparency, 2022 International Symposium on Antennas and Propagation (ISAP), 2022.
- [24] V. Kaim et al., Ultra-miniature circularly polarized CPW-fed implantable antenna design and its validation for biotelemetry applications, *Scientific Reports*, 10(1), 2020.
- [25] K. Kaur, A. Kumar and N. Sharma, A novel design of ultra-wideband CPW-fed printed monopole antenna for Wi-MAX, WLAN and X-band rejection characteristics, *Analog Integrated Circuits and Signal Processing*, 114(1), 2023.
- [26] R. Mali, D. Lodhi and S. Singhal, Quad broadband circularly polarized CPW FED cleaver-shaped extended UWB MIMO antenna for 5G, C, K and millimetre wave applications, *Analog Integrated Circuits and Signal Processing*, 2023.
- [27] S. Kiani, P. Rezaei and M. Fakhr, A CPW-fed wearable antenna at ISM band for biomedical and WBAN

- applications, *Wireless Networks*, 27(1), 2021, 735–745.
- [28] M.Y. Sai et al., CPW Fed Microstrip Patch Antenna for Dedicated Short-Range Communication, *Wireless Personal Communications*, 122(4), 2021, 3859–3873.
- [29] A.Kr. Yadav et al., Design and Analysis of CPW-Fed Antenna for Quad-Band Wireless Applications, *Journal of Electronic Materials*, 52(7), 2023, 4388–4399.
- [30] A.Kr. Yadav, S. Lata and S.Kr. Singh, Design and Investigation of a Double-Damru (Pellet Drum)-Shaped CPW-Fed Microstrip Patch Antenna for 5G Wireless Communications, *Journal of Electronic Materials*, 52(7), 2023, 4400–4412.
- [31] Md. M. Alam et al., A dual-band CPW-fed miniature planar antenna for S-, C-, WiMAX, WLAN, UWB, and X-band applications, *Scientific Reports*, 12(1), 2022.
- [32] J. Borah et al., Miniaturization and Optimization of FR4-Based CPW-fed Antenna for Multiband Applications, *Radio Electronics and Communications Systems*, 64(12), 2021, 660–668.
- [33] S.K. Singh, T. Sharan and A.K. Singh, Investigating the S-parameter ( $|S_{11}|$ ) of CPW-fed antenna using four different dielectric substrate materials for RF multiband applications, *AIMS Electronics and Electrical Engineering*, 6(3), 2022, 198–222.
- [34] S.N. Azemi et al., Gain Enhancement of CPW Antenna for IoT Applications using FSS with Miniaturized Unit Cell, *Journal of Physics: Conference Series*, 1962(1), 2021, 012052.
- [35] C. Ben Nsir et al., Design of a  $1 \times 2$  CPW Fractal Antenna Array on Plexiglas Substrate with Defected Ground Plane for Telecommunication Applications, *Engineering Technology & Applied Science Research*, 11(6), 2021, 7897–7903.
- [36] Y. Liu and K. Huang, CPW-fed circularly-polarized antenna array with high front-to-back ratio and low-profile, *Open Physics*, 16(1), 2018, 651–655.
- [37] A. Sharma et al., Design of CPW-Fed Antenna with Defected Substrate for Wideband Applications, *Journal of Electrical and Computer Engineering*, 2016, pp. 1–10.
- [38] D. Lodhi and S. Singhal, CPW-fed quasi-complementary super-wideband MIMO antenna, *Optical and Quantum Electronics*, 54(12), 2022.
- [39] M. Hussain et al., Bandwidth and Gain Enhancement of a CPW Antenna Using Frequency Selective Surface for UWB Applications, *Micromachines*, 14(3), 2023, p. 591.
- [40] K.G. Jangid et al., Triple-Notched Band CPW fed UWB Antenna with Metallic Reflector for High Gain Performance, *Advanced Electromagnetics*, 6(4), 2017, 15–21.
- [41] Z. Ding et al., A Novel Broadband Monopole Antenna with T-Slot, CB-CPW, Parasitic Stripe and Heart-Shaped Slice for 5G Applications, *Sensors*, 20(24), 2020, p. 7002.
- [42] Z. Ding, D. Zhang and C. Ma, Broadband Antenna Design with Integrated CB-CPW and Parasitic Patch Structure for WLAN, RFID, WiMAX, and 5G Applications, *IEEE Access*, 8, 2020, 42877–42883.
- [43] M. F. M. Omar, A. A. Manaf, M. F. Ain, S. K. A. Rahim et al., CPW-fed circular patch antenna with rectangular slot-loaded DGS for wideband application, *ELEKTRIKA*, 24(1), 2025, 7–13.
- [44] A.S. Priyadharshini, C. Arvind and M. Karthikeyan, Novel eng metamaterial for gain enhancement of an offset fed CPW concentric circle shaped patch antenna, *Wireless*

- Personal Communications, 130(4), 2023, 2515–2530.
- [45] P.S. Kumar and B.C. Mohan, Design of a miniaturized triple-band antenna with conductor-backed metasurfaces-CPW fed for 5G wireless applications, 2017 IEEE International Conference on Antenna Innovations & Modern Technologies for Ground, Aircraft and Satellite Applications (iAIM), 2017.
- [46] D. Negi and R. Khanna, A high-gain CPW-fed metamaterial antenna for UWB applications, Progress in Electromagnetics Research C, 132, 2023, 51–63.
- [47] M.F. Saad et al., CPW-UWB flexible composite antenna using jute textile for WPAN applications, 2020 IEEE International RF and Microwave Conference (RFM), 2020.
- [48] S. Aditya et al., High-gain 24-GHz CPW-fed microstrip patch antennas on high-permittivity substrates, IEEE Antennas and Wireless Propagation Letters, 3, 2004, 30–33.
- [49] K. Kaur, A. Kumar and N. Sharma, Split ring slot loaded compact CPW-fed printed monopole antennas for ultra-wideband applications with band Notch Characteristics, Progress in Electromagnetics Research C, 110, 2021, 39–54.
- [50] Y. Chen and C. Hsu, Inverted-E shaped monopole on high-permittivity substrate for application in industrial, scientific, medical, high-Performance Radio Local Area Network, unlicensed national information infrastructure, and worldwide interoperability for Microwave Access, IET Microwaves, Antennas & Propagation, 8(4), 2014, 272–277.
- [51] R. Teotia and T. Shanmuganatham, CPW-fed dodecagram fractal antenna with DGS for Multiband Applications, 2015 IEEE International Conference on Signal Processing, Informatics, Communication and Energy Systems (SPICES), 2015.
- [52] J. Gandhimohan and T. Shanmuganatham, CPW fed bud shaped antenna with DGS in UWB range for body area network, 2017 IEEE International Conference on Antenna Innovations and Modern Technologies for Ground, Aircraft and Satellite Applications (iAIM), 2017.
- [53] M. Dixit and M.G.S. Tripathi, CPW-fed monopole printed antenna using staircase shaped defected ground structure for wireless application, 2018 IEEE International Students' Conference on Electrical, Electronics and Computer Science (SCEECs), 2018.
- [54] M. Nosrati and N. Tavassolian, A wideband, high-gain, CPW-fed, circularly-polarized, L-shaped slot antenna array, 2017 IEEE International Symposium on Antennas and Propagation and USNC/URSI National Radio Science Meeting, 2017.
- [55] U. Farooq et al., Design of a 1×4 CPW microstrip antenna array on PET substrate for biomedical applications, 2019 IEEE International Symposium on Antennas and Propagation and USNC-URSI Radio Science Meeting, 2019.
- [56] H. Paik et al., High performance CPW fed printed antenna with double layered frequency selective surface reflector for bandwidth and gain improvement, Progress in Electromagnetics Research Letters, 102, 2022, 47–55.
- [57] W. Abbas Awan et al., A Frequency Selective Surface Loaded UWB Antenna for High Gain Applications, Computers, Materials & Continua, 73(3), 2022, 6169–6180.
- [58] G. Kumar, D. Singh, R. Kumar et al., A planar CPW fed UWB antenna with dual rectangular notch band

- characteristics incorporating U-slot, SRRs, and EBGs, *International Journal of RF and Microwave Computer-Aided Engineering*, 31(4), 2021, e22676.
- [59] A.S. Fazal et al., A compact UWB CPW-fed antenna with inverted L-shaped slot for WLAN band notched characteristics, 2017 11th European Conference on Antennas and Propagation (EUCAP), 2017.
- [60] G. Rajesh, R. Poonkuzhali, Design and analysis of CPW fed ultrathin flexible MIMO antenna for UWB and X-band applications, *IEEE Access*, 12, 2024, 96704–96713.
- [61] O. Elalaouy, M. EL Ghzaoui, J. Foshi, A high-isolated wideband two-port MIMO antenna for 5G millimeter-wave applications, *Results in Engineering*, 23, 2024, 102466.
- [62] S. Naik, A. Upmanyu, M. Sharma, Design and experimental analysis of asymmetric fed key-shaped eight-port flexible frequency diversity MIMO antenna with multi-band applications, *Optical and Quantum Electronics*, 57, 2025, 98.